THE JOURNAL OF PHYSICAL CHEMISTRY Letters

Letter

pubs.acs.org/JPCL

Importance of Polaronic Effects for Charge Transport in CdSe Quantum Dot Solids

Nikola Prodanović,*[,†,‡] Nenad Vukmirović,*[,‡] Zoran Ikonić,[†] Paul Harrison,[§] and Dragan Indjin[†]

[†]Institute of Microwaves and Photonics, School of Electronic and Electrical Engineering, University of Leeds, Woodhouse Lane, Leeds, LS2 9JT, United Kingdom

[‡]Scientific Computing Laboratory, Institute of Physics Belgrade, University of Belgrade, Pregrevica 118, 11080 Belgrade, Serbia

[§]Materials and Engineering Research Institute, Sheffield Hallam University, Sheffield, S1 1WB, United Kingdom

ABSTRACT: We developed an accurate model accounting for electron−phonon interaction in colloidal quantum dot supercrystals that allowed us to identify the nature of charge carriers and the electrical transport regime. We find that in experimentally analyzed CdSe nanocrystal solids, the electron−phonon interaction is sufficiently strong that small polarons localized to single dots are formed. Charge-carrier transport occurs by small polaron hopping between the dots, with mobility that decreases with increasing temperature. While such a temperature dependence of mobility is usually considered as a proof of band transport, we show that the same type of dependence occurs in the system where transport is dominated by small polaron hopping.

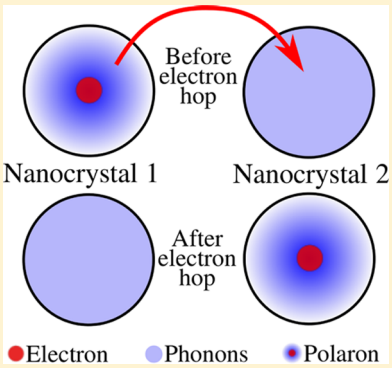

SECTION: Physical Processes in Nanomaterials and Nanostructures

Colloidal nanocrystals (NCs) exhibit electronic and optical properties that significantly differ from bulk semiconductors. Their electronic spectrum is discrete, defect density is low, and properties are size-tunable. In the past decade, special attention was given to arrays of NCs, i.e., nanocrystal solids (NSs).[1,2] Potential device applications of NSs include photodetection,[3] field effect transistors (FETs),[4] and photovoltaics.[5]

Good electronic transport between the NCs is required for efficient operation of all these devices. Initially, these structures exhibited very low conductivity, but increased interdot coupling by using shorter ligands and doping techniques enabled observable conductivity with corresponding mobility of the order of 10^{-2} $cm^2/(V\ s)$ (see ref 6). Conductivity decreased with the decreasing temperature indicating activated electron mobility. It was suggested[6] that Mott's variable range hopping[6−9] is the transport mechanism at low temperatures in these disordered, doped, and weakly coupled CdSe NCs.

A very strong effort has been put forth in order to achieve higher electron mobilities and band-like transport. In order to improve transport properties, the three main directions in technology development are fabrication of monodispersed systems, enhanced interdot coupling, and uniform high level doping. Despite the successes in the development of the technology, it is still a challenge to obtain NSs with high monodispersity and strong interdot coupling.[9,10] The upper limit of electron mobility presently is on the order of 10 $cm^2/(V\ s)$ (see refs 11−13). Such relatively high values of mobility, its decrease with increasing temperature, and absorption line width broadening upon formation of NS[12] were considered as a signature of band transport in these materials.

Numerous effects act detrimentally when band transport in realistic NSs is concerned, such as the effects of disorder[9] (nanocrystal size nonuniformity, irregularities in the spatial arrangement, nonuniform doping, etc), traps, and the electron−phonon interaction. While the effects of disorder and traps can be removed or significantly reduced at least in principle by the fabrication of high-quality structures, the electron−phonon interaction is intrinsic to the material and always ultimately exists. Despite this, very little is known about the strength of the electron−phonon interaction and its effect on transport properties in NSs. In an ideal NS, if the electron−phonon interaction in the NC were much weaker than electronic coupling between the NCs, the system would exhibit band transport where the electron−phonon interaction acts as a scattering mechanism that determines the value of the electron mobility. In the opposite limit, if the electron−phonon interaction were much stronger than the electronic coupling between the NCs, the formation of small polarons[14]—quasiparticles consisting of an electron in the NC dressed by phonons—would take place. In that case, the electronic coupling between the NCs acts as a perturbation that allows small polarons to hop from one NC to another, and such a transport regime is called small polaron hopping.[14,15] It is

Received: January 14, 2014
Accepted: February 21, 2014
Published: February 21, 2014

   dx.doi.org/10.1021/jz500086c | *J. Phys. Chem. Lett.* 2014, 5, 1335−1340

believed that small polaron hopping is the charge transport mechanism in a variety of materials such as atomic solids,[16] transition metal oxides,[17] and small molecule based organic semiconductors.[15]

In this work, we show that carrier transport in CdSe NSs at low carrier concentration occurs by small polaron hopping although the temperature dependence of mobility exhibits a band-like behavior. We calculate the strength and study the role of the electron−phonon interaction on the transport properties of carriers in NSs. Colloidal NCs, made of extremely polar semiconductors, exhibit strong electron−phonon interaction via polar coupling to optical phonons, which leads to small polaron formation. We calculate the mobility of small polarons, which in the relevant range of temperatures exhibits a decrease with increasing temperature. This implies that a decrease of mobility with increasing temperature cannot be considered as a signature of band transport.

We consider an ideal cubic lattice of NCs with lattice constant C. Each NC is assumed to have the shape of a sphere with radius a in the 2.0−4.0 nm range[8,10] that provides three-dimensional confinement for electrons with infinitely high potential barrier. We assume interdot spacing of d = 1 nm, which gives $C = 2a + d$ (see Figure 1).

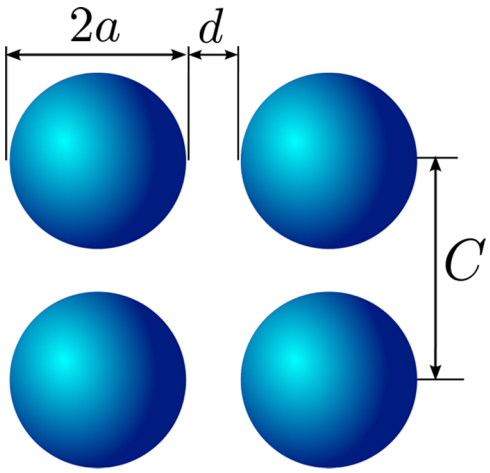

Figure 1. 2D sketch of a colloidal nanocrystal solid with nanocrystal radius a, interdot spacing d, and lattice constant C.

The electronic structure of a NC is considered within the effective mass approximation. The energy separation between s-like ground and p-like first excited states in the conduction band is above 200 meV for all realistic values of dot radius a. Therefore we assume that transport at low carrier concentration, where the effects of charging[8,18−20] are negligible, occurs only through ground s-like states, since these are the only ones that are significantly populated. Within the effective mass approximation, the s-like wave function of the ground state is given as

$$\psi(\mathbf{r}) = \sqrt{\frac{1}{2\pi a^3 j_1^2(\alpha_{00})}}\, j_0\left(\frac{\alpha_{00}}{a} r\right) \tag{1}$$

where j_n is the spherical Bessel function of order n and α_{00} is the first zero of j_0.

Electronic coupling between ground states of neighboring NCs depends on various factors, such as the dot size, the interdot spacing, the type of ligands at the surface of the dots, as well as on the linker molecules that can be used to increase the coupling between the dots.[4,21−25] Recent ab initio calculations[21] have shown that electronic coupling in CdSe NCs linked with the Sn_2S_6 molecule strongly depends on the dot size and the type of molecule attachment and takes the values below 10 meV for dots with the radius above 2 nm. The electronic coupling between dots depends on many factors, and as a parameter that can be technologically engineered, it is appropriate to use it as an input free parameter in the following theoretical consideration.

To model the interaction of electrons with phonons in the NC, we consider longitudinal optical (LO) modes that couple to electrons via polar coupling and acoustic modes, which couple to electrons via deformation potential and piezoelectric coupling.

We use the dielectric continuum model given in refs 26−29 to model the optical confined modes, their frequencies, and their coupling to electronic states. This model gives two groups of optical confined modes: the LO modes and the surface optical (SO) modes.[26] Due to the spherical symmetry of the electron wave function, only LO modes couple with electrons in the ground state.

The elastic continuum model is used to model acoustic confined modes as in ref 30. Two types of modes arise from such a model: spheroidal and torsional modes. Spheroidal modes have longitudinal component, while torsional modes are fully transversal modes. Only spheroidal modes couple to electrons via deformation potential regardless of the electronic state. It turns out that torsional modes do not couple to the ground state via piezoelectric coupling due to its spherical symmetry. Therefore only spheroidal modes are relevant.

We include in the Hamiltonian a limited number of phonon modes with the strongest coupling to electrons by choosing the modes with the largest ratio of electron−phonon coupling G_f and phonon energy $\hbar\Omega_f$. Selected modes and corresponding parameters are presented in Table 1. The inclusion of additional modes has no significant effect on the results that will be presented.

Table 1. Phonon Energies $\hbar\Omega$ and Electron−Phonon Coupling Constants to the Electronic Ground State G in a CdSe NC for Different Values of the Dot Radius

mode types →	acoustic spheroidal		acoustic spheroidal		acoustic spheroidal		acoustic spheroidal		longitudinal optical		longitudinal optical	
parameters [meV] →	$\hbar\Omega_1$	G_1	$\hbar\Omega_2$	G_2	$\hbar\Omega_3$	G_3	$\hbar\Omega_4$	G_4	$\hbar\Omega_5$	G_5	$\hbar\Omega_6$	G_6
1.8 nm	3.78	−2.82	8.10	−0.14	1.46	−0.78	2.87	0.52	24.00	20.33	24.00	3.52
2.0 nm	3.40	−2.40	7.29	−0.05	1.32	−0.70	2.60	0.46	24.00	19.28	24.00	3.34
2.5 nm	2.72	−1.72	5.83	0.07	1.05	−0.56	2.08	0.37	24.00	17.25	24.00	2.97
3.0 nm	2.27	−1.32	4.86	0.12	0.88	−0.47	1.73	0.31	24.00	15.75	24.00	2.73
3.5 nm	1.95	−1.06	4.16	0.14	0.75	−0.40	1.48	0.27	24.00	14.58	24.00	2.52

dx.doi.org/10.1021/jz500086c | J. Phys. Chem. Lett. 2014, 5, 1335−1340

We find that confined LO phonon modes at energies of 24 meV are responsible for the strongest electron−phonon coupling constants on the order of 15−20 meV. These values are significantly larger than typical electronic transfer integrals, which gives a first indication that small polaron formation might take place. Having the importance of the values of electron−LO phonon coupling constants in mind, we have checked that they are reasonable by also computing them using the bulk phonon model and taking the standard expression for Fröhlich coupling. The root of the sum of all electron−LO phonon coupling constants squared is in the range 20−30 meV within the bulk phonon model, and in the 15−20 meV range within the confined phonon model for the value of radius in the 3.5−1.8 nm range. The similarity of these values suggests that the values of electron−LO phonon coupling constants obtained from the model that we used are in accordance with expectations.

With the obtained phonon modes, frequencies, and coupling strengths, one can construct the Hamiltonian of an infinite three-dimensional NS:

$$\hat{H} = \hat{H}_{\mathrm{e}} + \hat{H}_{\mathrm{ph}} + \hat{H}_{\mathrm{e-ph}} \tag{2}$$

where

$$\hat{H}_{\mathrm{e}} = \sum_{\mathbf{RS}} J_{\mathbf{R-S}} \hat{A}_{\mathbf{R}}^{\dagger} \hat{A}_{\mathbf{S}} \tag{3}$$

$$\hat{H}_{\mathrm{ph}} = \bar{h} \sum_{\mathbf{R},f} \Omega_f \hat{B}_{\mathbf{R},f}^{\dagger} \hat{B}_{\mathbf{R},f} \tag{4}$$

$$\hat{H}_{\mathrm{e-ph}} = \sum_{\mathbf{R},f} G_f \hat{A}_{\mathbf{R}}^{\dagger} \hat{A}_{\mathbf{R}} (\hat{B}_{\mathbf{R},f}^{\dagger} + \hat{B}_{\mathbf{R},f}) \tag{5}$$

In the previous equations $\hat{A}_{\mathbf{R}}^{\dagger}$ and $\hat{A}_{\mathbf{R}}$ are the creation and annihilation operators for an electron in NC at site **R**, $\hat{B}_{\mathbf{R},f}^{\dagger}$ and $\hat{B}_{\mathbf{R},f}$ are the corresponding operators for a mode f phonon in NC at the same site, while $J_{\mathbf{R-S}}$ is electronic coupling (electronic transfer integral) between the ground states of NCs at sites **R** and **S**. We include only the coupling between nearest neighbors because electronic coupling between more remote neighbors is negligibly small.[18]

To establish the nature of charge carriers described by this Hamiltonian and their transport regime, we follow the variational polaron approach as in refs 31 and 32. We apply the Merrifield's unitary transformation of the Hamiltonian $\hat{H}(\mathbf{D}) = \hat{U}^{-1}(\mathbf{D})\hat{H}\hat{U}(\mathbf{D})$, where

$$\hat{U}(\mathbf{D}) = e^{\sum_{\mathbf{R}} \hat{A}_{\mathbf{R}}^{\dagger}\hat{A}_{\mathbf{R}} \sum_{\mathbf{S},f} D_{\mathbf{S},f}(\hat{B}_{\mathbf{R}+\mathbf{S},f} - \hat{B}_{\mathbf{R}+\mathbf{S},f}^{\dagger})} \tag{6}$$

The transformed Hamiltonian is of the form $\hat{H}(\mathbf{D}) = \hat{H}_0(\mathbf{D}) + \hat{V}(\mathbf{D})$, where $\hat{H}_0(\mathbf{D})$ describes noninteracting polarons and phonons, while $\hat{V}(\mathbf{D})$ contains the interaction between phonons and polarons. This interaction acts only as perturbation if the $D_{\mathbf{S},f}$ coefficients are chosen appropriately. The coefficients $D_{\mathbf{S},f}$ in the unitary transformation are obtained from the condition that Bogoliubov upper bound on the free energy of the Hamiltonian $\hat{H}(\mathbf{D})$ is minimal.[32]

The coefficients $D_{\mathbf{S},f}$ quantify the degree of dressing of an electron at site **R** by phonon of mode f at site **R** + **S**. In the case of strong electron−phonon interaction, the electrons are dressed by phonons from the same site, and these coefficients take the form $D_{\mathbf{S},f} = \delta_{\mathbf{S},0}(G_f)/(\bar{h}\Omega_f)$. On the other hand, for a weak electron−phonon interaction, these coefficients have smaller values, but their range is much longer, and phonons from many different sites participate in dressing the electron. Therefore, one can in principle define that the charge carrier is a small polaron if the dependence of $D_{\mathbf{S},f}$ on **S** is strongly peaked at **S** = 0.

It is, however, more convenient to have a single number that describes whether the carriers are small polarons or not. The electron−phonon interaction also leads to renormalization of the band dispersion from the $E_{\mathbf{k}} = \Sigma_{\mathbf{R}} J_{\mathbf{R}} e^{i\mathbf{k}\cdot\mathbf{R}}$ to the $E_{\mathbf{k}}(\mathbf{D}) = \Sigma_{\mathbf{R}} J_{\mathbf{R}}(\mathbf{D}) e^{i\mathbf{k}\cdot\mathbf{R}} + E'(\mathbf{D})$ dependence, where

$$J_{\mathbf{R}}(\mathbf{D}) = J_{\mathbf{R}} e^{-1/2 \sum_{\mathbf{R}',f} (D_{\mathbf{R}',f} - D_{\mathbf{R}'-\mathbf{R},f})^2 \coth(\frac{\beta\hbar\Omega_f}{2})} \tag{7}$$

and

$$E'(\mathbf{D}) = \sum_f \left(\sum_{\mathbf{R}} \bar{h}\Omega_f D_{\mathbf{R},f}^2 - 2G_f D_{0,f} \right) \tag{8}$$

with $\beta = 1/(k_{\mathrm{B}}T)$, where T is the temperature. The term $E'(\mathbf{D})$ does not depend on wavevector **k**, and can be further omitted from discussion. Therefore, the electron−phonon interaction leads to the reduction of the bandwidth by a factor of $\kappa = J_{\mathbf{R}}(\mathbf{D})/J_{\mathbf{R}}$ (In the case of nearest neighbor approximation, κ is unambiguously defined). If the carriers are small polarons, then the condition $\kappa \ll 1$ is satisfied.[32] In Figure 2 we present values

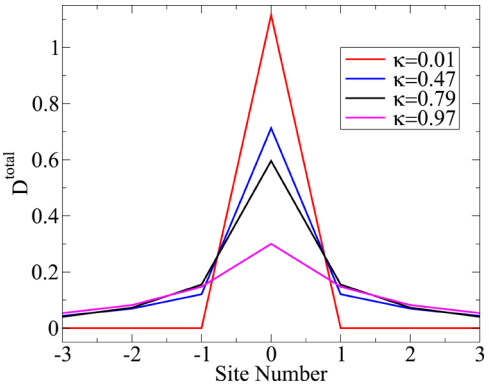

Figure 2. $D_{\mathbf{R}}^{\mathrm{total}} = (\Sigma_f D_{\mathbf{R},f}^2)^{1/2}$ for 1D lattice model (with dot radius 2.5 nm) for several values of parameter κ. The phonon spectrum is taken from Table 1. The value of $\kappa = 0.97$ corresponds to $J = -25$ meV and $T = 4$ K, $\kappa = 0.79$ corresponds to $J = -6.4$ meV and $T = 4$ K, $\kappa = 0.47$ corresponds to $J = -6.4$ meV and $T = 162$ K, $\kappa = 0.01$ corresponds to $J = -6.4$ meV and $T = 240$ K.

of variational parameters averaged over all phonon modes in terms of integer lattice site and for several values of parameter κ. For maximal value of $\kappa \approx 1$, variational parameters exhibit significant values for relatively far sites. With decreasing κ, the central coefficient becomes larger, but the coefficients far from the central site decrease. Eventually, for $\kappa \approx 0$, parameters are strongly peaked at **S** = 0, and the formation of a small polaron takes place. Consequently, we introduce the criterion $\kappa < 0.05$, which can be used as a threshold beyond which the small polaron formation takes place, as indicated in Figure 2.

In Figure 3 we present for several different values of dot radius the region of (J,T) parameters for which the condition $\kappa < 0.05$ is satisfied. These results demonstrate that at room temperature the charge carriers in NSs are small polarons for all realistic values of electronic coupling and dot dimensions. Namely, as seen from Figure 3, electronic coupling of at least 10 meV for nanocrystals with the radius of about 2 nm would be required to break the small polaron at room temperature, a

dx.doi.org/10.1021/jz500086c | J. Phys. Chem. Lett. 2014, 5, 1335−1340

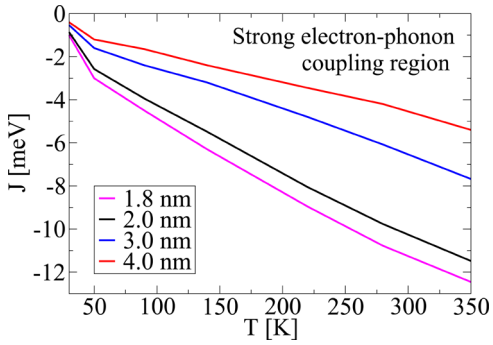

Figure 3. J versus T diagram demonstrating the area of strong electron−phonon coupling regime for several dot sizes. The dot radius is specified in the legend. The limiting curve has been defined by the condition $\kappa < 0.05$. Strong electron−phonon coupling regime occurs in the upper right region of the diagram.

value much larger then theoretical[21] and experimental[12] estimates of electronic coupling for 2 nm radius nanocrystals. For larger nanocrystals, somewhat smaller values of electronic coupling ranging from 4 to 10 meV are required to break the small polaron. However, theoretical predictions[21] indicate that electronic coupling in these nanocrystals is significantly smaller than that.

Next, we calculate the charge carrier mobility when the system is in the small polaron regime. The mobility is given from the Einstein relation as $\mu = \beta De$, where D is the diffusion constant. The diffusion constant can be expressed in terms of the small polaron hopping rate W between two neighboring dots as $D = WC^2$. The expression for the small polaron hopping rate is given as[33,34]

$$W = \frac{J^2}{\bar{h}^2}\int_{-\infty}^{\infty} dt\, \exp\left\{-2\sum_f \frac{G_f^2}{(\bar{h}\Omega_f)^2} \times [(2N_f+1) - (N_f+1)e^{-i\Omega_f t} - N_f e^{i\Omega_f t}]\right\} \quad (9)$$

In the high-temperature limit $\beta\bar{h}\Omega_f \ll 1$, this expression reduces to the well-known Marcus formula

$$W = \frac{J^2}{\bar{h}}\sqrt{\frac{\beta\pi}{\lambda}}\, e^{-\beta\lambda/4} \quad (10)$$

where $\lambda = 2\Sigma_f(G_f^2)/(\bar{h}\Omega_f)$ is the reorganization energy. However, for the electron−phonon coupling strengths given in Table 1, the high-temperature limit condition is not satisfied, and therefore we use eq 9 instead of the simpler eq 10. Equation 9 can alternatively be obtained by applying Kubo's linear response theory to transformed Hamiltonian and taking the limit of strong electron−phonon coupling.[35] Therefore, this is a full quantum mechanical formula for charge carrier mobility.

In our model, we have not included the effects of polarization of the surrounding dielectric during charge carrier hopping between the dots. These effects are typically modeled using external reorganization energy given as[36−38]

$$\lambda_{ext} = \frac{e^2}{4\pi\varepsilon_0}\left(\frac{1}{a} - \frac{1}{C}\right)\left(\frac{1}{\varepsilon_\infty} - \frac{1}{\varepsilon_{st}}\right) \quad (11)$$

where ε_∞ and ε_{st} are the static and high frequency relative dielectric constant of the surrounding dielectric. For an estimate of the value of λ_{ext}, we take the CdSe values ε_∞ = 6.9 and ε_{st} = 9.6 (a more accurate treatment would involve the use of an effective medium theory to calculate the effective dielectric constant of the dot surroundings) and obtain that λ_{ext} takes the values from the (8−18) meV range. External reorganization energy could be phenomenologically added to our model through the $e^{-\beta\lambda_{ext}/4}$ term that multiplies the hopping rate as follows from eq 10. We estimated that this term has a weak effect on the temperature dependence of the mobility.

The calculated temperature dependence of the mobility for several dot sizes and electronic coupling parameters is presented in Figure 4. In all these cases, the small polaron

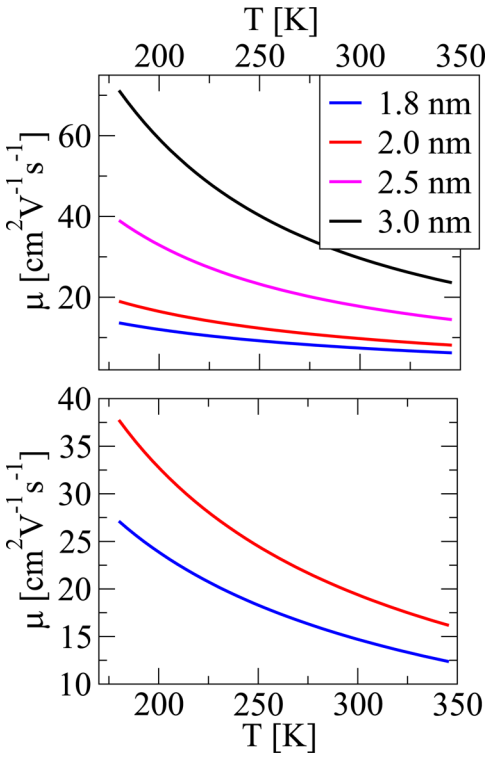

Figure 4. Mobility vs temperature plot for various dot radii and two different values of electronic coupling between the dots. The upper plot corresponds to $J = -3.9$ meV and the calculated mobility for the 2 nm dot resembles that from ref 11. The lower part of the figure corresponds to $J = -5.5$ meV and the calculated mobility for the 2 nm dot resembles that from ref 12 (Figure 4b). In both ref 11 and ref 12, the estimated dot radius is about 2 nm.

condition is satisfied, as can be seen from Figure 3. We find that in the range of temperatures around room temperature, the mobility decreases with increasing temperature for all the investigated dot dimensions. Such a temperature dependence was, in several previous works,[11−13] considered to be a signature of band transport (along with the absorption line width broadening upon the formation of NS[12]). Here, we demonstrate that this type of temperature dependence is present also in small polaron transport. Therefore, the "band-like" temperature dependence of the mobility cannot be considered as a proof of band transport. In fact, we have shown that electron−phonon interaction in CdSe dots is sufficiently strong for the formation of small polarons whose mobility decreases with increasing temperature.

dx.doi.org/10.1021/jz500086c | J. Phys. Chem. Lett. 2014, 5, 1335−1340

The mobility that decreases with increasing temperature is somewhat unexpected for hopping transport. The mobility is proportional to the W/T ratio and we find that its temperature dependence is dominated by the T factor in the denominator. Physical origin of the T factor is the fact that mobility describes the directed drift motion which is suppressed at higher temperatures over the random diffusive motion (as quantified by the Einstein formula). As far as temperature dependence of W is concerned, we find that it slightly decreases with increasing temperature. In the semiclassical Marcus picture of carrier hopping, the exponential term in Marcus formula originates from the energy barrier required for the carrier to cross from the potential surface of one dot to another. The temperature dependent prefactor originates from the fact that at higher temperatures the electron moves faster and spends less time in the crossing region of potential surfaces; this effect decreases its hopping probability from one surface to another. The temperature dependences due to these two terms in the Marcus formula nearly cancel each other in our system.

We also find that the strength of the electron−phonon coupling influences the mobility. By increasing the dot size, the strength of the electron−phonon coupling decreases, and the mobility increases as presented in Figure 4. This is an expected behavior for the small polaron regime because weaker electron−phonon coupling leads to a polaron that is less strongly bound and therefore it can hop to a neighboring dot more easily. An increase of mobility with an increase in dot dimensions has been observed in several experiments.[22,39] In the small polaron regime, the mobility has quadratic dependence on electronic coupling J, which is a direct consequence of eq 9.

In ref 12, the mobilities of the order of 20−30 $cm^2/(V\ s)$ were measured in the linear regime in field-effect transistors with CdSe NSs. These mobilities gradually increase, exhibit a peak (around 150 K for the sample at bottom panel in Figure 4b in ref 12) and then gradually decrease with increasing temperature. We reproduce the decreasing behavior at temperatures above 150 K (Figure 4), while the increasing part in ref 12 originates from thermally activated transport due to shallow traps which are not included in our model. One should still note that the comparison of our calculations with these experiments should be taken with caution due to the effects of disorder and traps which are present in experiment. We stress again that despite the relatively large values of mobility, for these parameters, the electrical transport takes place by small polaron hopping.

Next, we discuss other well-known effects in the system which may lead to charge carrier localization and hopping transport. The effects of disorder can cause Anderson localization[40,41] of wave functions, which lead to vanishing conductivity at zero temperature and thermally activated hopping at finite temperatures.[41] On the other hand, at higher carrier concentrations, the effects of electron−electron interaction become important and may also lead to carrier localization and formation of a Mott insulator.[42] Our results indicate that in the absence of disorder and electron−electron interactions, electron−phonon interaction is sufficiently strong to lead to the formation of localized small polarons, which exhibit hopping transport.

Realistic NSs are certainly disordered to some extent and contain some traps.[43] Since the main conclusion of our paper is that electron−phonon interaction is already sufficient to localize the carriers (which leads to hopping transport) and both disorder and traps also act to localize the carrier, their presence will certainly not change the transport mechanism in the system.

In summary, we have developed a model to describe the electronic transport at low carrier concentration in ideal NSs. We have used elastic and dielectric continuum models to obtain phonon spectra and the strength of their coupling to electrons. Variational polaron theory was then used to establish the nature of charge carriers. Hopping rates and carrier mobility were evaluated using the approach that fully takes into account the quantum mechanical nature of phonons and their interaction with electrons.

We have identified the conditions for the strong coupling regime where band narrowing is so strong that small polaron formation takes place. Based on this and calculated mobilities, we conclude that recently fabricated NSs do not exhibit band transport but instead reside in the strong electron−phonon coupling regime where localized carriers exhibit hopping transport. In such a transport regime, the mobility also decreases by increasing the temperature.

AUTHOR INFORMATION

Corresponding Authors

*E-mail: nikola.prodanovic@ipb.ac.rs.

*E-mail: nenad.vukmirovic@ipb.ac.rs.

Notes

The authors declare no competing financial interest.

ACKNOWLEDGMENTS

N.P. acknowledges the support in part by the University of Leeds Fully Funded International Research Scholarships program and in part by the Ministry of Education and Science, Republic of Serbia, Scholarship program for students studying at the world's leading universities. N.V. was supported by the European Community FP7 Marie Curie Career Integration Grant (ELECTROMAT), Serbian Ministry of Education, Science and Technological Development (Project ON171017), and FP7 Projects PRACE-2IP, PRACE-3IP, and EGI-InSPIRE. D.I., Z.I., and P.H. acknowledge support of the NATO Science for Peace and Security Project EAP.SFPP 984068 and European Cooperation in Science and Technology (COST) Actions BM1205 and MP1204.

REFERENCES

(1) Murray, C. B.; Kagan, C. R.; Bawendi, M. G. Self-Organization of CdSe Nanocrystallites into Three-Dimensional Quantum Dot Superlattices. *Science* **1995**, *270*, 1335−1338.

(2) Roest, A. L.; Kelly, J. J.; Vanmaekelbergh, D. Coulomb Blockade of Electron Transport in a ZnO Quantum-Dot Solid. *Phys. Lett. A* **2003**, *83*, 5530−5532.

(3) Ginger, D. S.; Greenham, N. C. Charge Injection and Transport in Films of CdSe Nanocrystals. *J. Appl. Phys.* **2000**, *87*, 1361−1368.

(4) Talapin, D. V.; Murray, C. B. PbSe Nanocrystal Solids for n- and p-Channel Thin Film Field-Effect Transistors. *Science* **2005**, *310*, 86−89.

(5) Sargent, E. H. Infrared Photovoltaics Made by Solution Processing. *Nat. Photonics* **2009**, *3*, 325−331.

(6) Yu, D.; Wang, C.; Wehrenberg, B. L.; Guyot-Sionnest, P. Variable Range Hopping Conduction in Semiconductor Nanocrystal Solids. *Phys. Rev. Lett.* **2004**, *92*, 216802.

(7) Mott, N. F.; Davis, E. A. *Electronic Processes in Non-Crystalline Materials*, 2nd ed.; Clarendon Press: Oxford, U.K., 1979.

(8) Skinner, B.; Chen, T.; Shklovskii, B. I. Theory of Hopping Conduction in Arrays of Doped Semiconductor Nanocrystals. *Phys. Rev. B* **2012**, *85*, 205316.
(9) Guyot-Sionnest, P. Electrical Transport in Colloidal Quantum Dot Films. *J. Phys. Chem. Lett.* **2012**, *3*, 1169−1175.
(10) Talapin, D. V.; Lee, J.-S.; Kovalenko, M. V.; Shevchenko, E. V. Prospects of Colloidal Nanocrystals for Electronic and Optoelectronic Applications. *Chem. Rev.* **2010**, *110*, 389−458.
(11) Lee, J.-S.; Kovalenko, M. V.; Huang, J.; Chung, D. S.; Talapin, D. V. Band-like Transport, High Electron Mobility and High Photoconductivity in All-Inorganic Nanocrystal Arrays. *Nat. Nanotechnol.* **2011**, *92*, 348−352.
(12) Choi, J.-H.; Fafarman, A. T.; Oh, S. J.; Ko, D.-K.; Kim, D. K.; Diroll, B. T.; Muramoto, S.; Gillen, J. G.; Murray, C. B.; Kagan, C. R. Bandlike Transport in Strongly Coupled and Doped Quantum Dot Solids: A Route to High-Performance Thin-Film Electronics. *Nano Lett.* **2012**, *12*, 2631−2638.
(13) Talgorn, E.; Gao, Y.; Aerts, M.; Kunneman, L. T.; Schins, J. M.; Savenije, T. J.; van Huis, M. A.; van der Zant, H. S. J.; Houtepen, A. J.; Siebbeles, L. D. A. Unity Quantum Yield of Photogenerated Charges and Band-like Transport in Quantum-Dot Solids. *Nat. Nanotechnol.* **2011**, *6*, 733−739.
(14) Holstein, T. Studies of Polaron Motion. *Ann. Phys.* **1959**, *8*, 343−359.
(15) Troisi, A. Charge Transport in High Mobility Molecular Semiconductors: Classical Models and New Theories. *Chem. Soc. Rev.* **2011**, *40*, 2347−2358.
(16) Le Comber, P. G.; Loveland, R. J.; Spear, W. E. Hole Transport in the Rare-gas Solids Ne, Ar, Kr, and Xe. *Phys. Rev. B* **1975**, *11*, 3124−3130.
(17) Hartinger, C.; Mayr, F.; Deisenhofer, J.; Loidl, A.; Kopp, T. Large and Small Polaron Excitations in $La_{2/3}(Sr/Ca)_{1/3}MnO_3$ Films. *Phys. Rev. B* **2004**, *69*, 100403.
(18) Lepage, H.; Kaminski-Cachopo, A.; Poncet, A.; le Carval, G. Simulation of Electronic Transport in Silicon Nanocrystal Solids. *J. Phys. Chem. C* **2012**, *116*, 10873−10880.
(19) van de Lagemaat, J. Einstein Relation for Electron Diffusion on Arrays of Weakly Coupled Quantum Dots. *Phys. Rev. B* **2005**, *72*, 235319.
(20) Chandler, R. E.; Houtepen, A. J.; Nelson, J.; Vanmaekelbergh, D. Electron Transport in Quantum Dot Solids: Monte Carlo Simulations of the Effects of Shell Filling, Coulomb Repulsions, and Site Disorder. *Phys. Rev. B* **2007**, *75*, 085325.
(21) Chu, I.-H.; Radulaski, M.; Vukmirovic, N.; Cheng, H.-P.; Wang, L.-W. Charge Transport in a Quantum Dot Supercrystal. *J. Phys. Chem. C* **2011**, *115*, 21409−21415.
(22) Liu, Y.; Gibbs, M.; Puthussery, J.; Gaik, S.; Ihly, R.; Hillhouse, H. W.; Law, M. Dependence of Carrier Mobility on Nanocrystal Size and Ligand Length in PbSe Nanocrystal Solids. *Nano Lett.* **2010**, *10*, 1960−1969.
(23) Fafarman, A. T.; Koh, W.-k.; Diroll, B. T.; Kim, D. K.; Ko, D.-K.; Oh, S. J.; Ye, X.; Doan-Nguyen, V.; Crump, M. R.; Reifsnyder, D. C.; et al. Thiocyanate-Capped Nanocrystal Colloids: Vibrational Reporter of Surface Chemistry and Solution-Based Route to Enhanced Coupling in Nanocrystal Solids. *J. Am. Chem. Soc.* **2011**, *133*, 15753−15761.
(24) Kovalenko, M. V.; Scheele, M.; Talapin, D. V. Colloidal Nanocrystals with Molecular Metal Chalcogenide Surface Ligands. *Science* **2009**, *324*, 1417−1420.
(25) Tang, J.; Kemp, K. W.; Hoogland, S.; Jeong, K. S.; Liu, H.; Levina, L.; Furukawa, M.; Wang, X.; Debnath, R.; Cha, D.; et al. Colloidal-Quantum-Dot Photovoltaics Using Atomic-Ligand Passivation. *Nat. Mater.* **2011**, *10*, 765−771.
(26) Klein, M. C.; Hache, F.; Ricard, D.; Flytzanis, C. Size Dependence of Electron-phonon Coupling in Semiconductor Nanospheres: The Case of CdSe. *Phys. Rev. B* **1990**, *42*, 11123−11132.
(27) Stroscio, M. A. *Phonons in Nanostructures*; Cambridge University Press: Cambridge, U.K., 2004.
(28) Licari, J. J.; Evrard, R. Electron−Phonon Interaction in a Dielectric Slab: Effect of the Electronic Polarizability. *Phys. Rev. B* **1977**, *15*, 2254−2264.
(29) Mori, N.; Ando, T. Electron−Optical-Phonon Interaction in Single and Double Heterostructures. *Phys. Rev. B* **1989**, *40*, 6175−6188.
(30) Takagahara, T. Electron−Phonon Interactions in Semiconductor Nanocrystals. *J. Lumin.* **1996**, *70*, 129−143.
(31) Yarkoni, D. R.; Silbey, R. J. Variational Approach to Exciton Transport in Molecular Crystals. *J. Chem. Phys.* **1977**, *67*, 5818−5827.
(32) Cheng, Y.-C.; Silbey, R. J. A Unified Theory for Charge-Carrier Transport in Organic Crystals. *J. Chem. Phys.* **2008**, *128*, 114713.
(33) Lin, S. H.; Chang, C. H.; Liang, K. K.; Chang, R.; Shiu, Y. J.; Zhang, J. M.; Yang, T.-S.; Hayashi, M.; Hsu, F. C. Ultrafast Dynamics and Spectroscopy of Bacterial Photosynthetic Reaction Centers. *Adv. Chem. Phys.* **2002**, *121*, 1−88.
(34) Nan, G.; Yang, X.; Wang, L.; Shuai, Z.; Zhao, Y. Nuclear Tunneling Effects of Charge Transport in Rubrene, Tetracene, and Pentacene. *Phys. Rev. B* **2009**, *79*, 115203.
(35) Ortmann, F.; Bechstedt, F.; Hannewald, K. Theory of Charge Transport in Organic Crystals: Beyond Holstein's Small-Polaron Model. *Phys. Rev. B* **2009**, *79*, 235206.
(36) Marcus, R. A. On the Theory of Oxidation-Reduction Reactions Involving Electron Transfer. I. *J. Chem. Phys.* **1956**, *24*, 966−978.
(37) Lepage, H.; Kaminski-Cachopo, A.; Poncet, A.; le Carval, G. Simulation of Electronic Transport in Silicon Nanocrystal Solids. *J. Phys. Chem. C* **2012**, *116*, 10873−10880.
(38) Vaissier, V.; Barnes, P.; Kirkpatrick, J.; Nelson, J. Influence of Polar Medium on the Reorganization Energy of Charge Transfer Between Dyes in a Dye Sensitized Film. *Phys. Chem. Chem. Phys.* **2013**, *15*, 4804−4814.
(39) Kang, M. S.; Sahu, A.; Norris, D. J.; Frisbie, C. D. Size-Dependent Electrical Transport in CdSe Nanocrystal Thin Films. *Nano Lett.* **2010**, *10*, 3727−3732.
(40) Anderson, P. W. Absence of Diffusion in Certain Random Lattices. *Phys. Rev.* **1958**, *109*, 1492−1505.
(41) Mott, N. F. *Metal-Insulator Transitions*; Taylor and Francis: London, 1990.
(42) Gebhard, F. *The Mott Metal−Insulator Transition*; Springer: Berlin, 1997.
(43) Zhitomirsky, D.; Kramer, I. J.; Labelle, A. J.; Fischer, A.; Debnath, R.; Pan, J.; Bakr, O. M.; Sargent, E. H. Colloidal Quantum Dot Photovoltaics: The Effect of Polydispersity. *Nano Lett.* **2012**, *12*, 1007−1012.